J Physiol Sci (2012) 62:221–231
DOI 10.1007/s12576-012-0200-4

ORIGINAL PAPER

Evaluation of left ventricular mechanical work and energetics of normal hearts in SERCA2a transgenic rats

Guo-Xing Zhang · Koji Obata · Daisuke Takeshita · Shinichi Mitsuyama · Tamiji Nakashima · Akio Kikuta · Masumi Hirabayashi · Koichi Tomita · Roland Vetter · Wolfgang H. Dillmann · Miyako Takaki

Received: 1 February 2012 / Accepted: 9 February 2012 / Published online: 1 March 2012

Abstract Cardiac sarcoplasmic reticulum (SR) Ca^{2+}-ATPase (SERCA2a) is responsible for most of the Ca^{2+} removal during diastole and a larger Ca^{2+} handling energy consumer in excitation–contraction (E–C) coupling. To understand the cardiac performance under long-term SERCA2a overexpression conditions, we established SERCA2a transgenic (TG) Wistar rats to analyze cardiac mechanical work and energetics in normal hearts during pacing at 300 beats/min. SERCA2a protein expression was increased in TGI and TGII rats (F2 and F3 of the same father and different mothers). Mean left ventricular (LV) end-systolic pressure (ESP) and systolic pressure–volume area (PVA; a total mechanical energy per beat) at midrange LV volume (mLVV) were significantly larger in TGI rats and were unchanged in TGII rats, compared to those in non-TG [wildtype (WT)] littermates. Mean myocardial oxygen consumption per minute for E–C coupling was significantly increased, and the mean slope of myocardial oxygen consumption per beat (VO_2)–PVA (systolic PVA) linear relation was smaller, but the overall O_2 cost of LV contractility for Ca^{2+} is unchanged in all TG rats. Mean Ca^{2+} concentration exerting maximal ESP_{mLVV} in TGII rats was significantly higher than that in WT rats. The Ca^{2+} overloading protocol did not elicit mitochondrial swelling in TGII rats. Tolerance to higher Ca^{2+} concentrations may support the possibility for enhanced SERCA2a activity in TGII rats. In conclusion, long-term SERCA2a overexpression enhanced or maintained LV mechanics, improved contractile efficiency under higher energy expenditure for Ca^{2+} handling, and improved Ca^{2+} tolerance, but it did not change the overall O_2 cost of LV contractility for Ca^{2+} in normal hearts of TG rats.

Keywords Pressure–volume area · SERCA2a · Transgenic rat

G.-X. Zhang and K. Obata contributed equally to this work.

G.-X. Zhang · K. Obata · D. Takeshita · S. Mitsuyama · M. Takaki (✉)
Department of Physiology II, Nara Medical University School of Medicine, 840 Shijo-cho, Kashihara, Nara 634-8521, Japan
e-mail: mtakaki@naramed-u.ac.jp

G.-X. Zhang
Department of Physiology, Medical College of Soochow University, Dushu Lake Campus, Suzhou Industrial Park, Suzhou 215123, People's Republic of China

T. Nakashima · A. Kikuta
Department of Anatomy, School of Medicine, University of Occupational and Environmental Health, Kitakyushu 807-8555, Japan

M. Hirabayashi · K. Tomita
National Institute for Physiological Sciences, Okazaki, Aichi 444-8787, Japan

R. Vetter
Institut für Klinische Pharmakologie und Toxikologie, Charité-Universitätsmedizin Berlin, Charité Campus Mitte, Hufelandweg 9, 10117 Berlin, Germany

W. H. Dillmann
Department of Medicine, University of California, San Diego, La Jolla, CA, USA

Introduction

Calcium (Ca^{2+}) homeostasis plays a critical role in maintaining physiological cardiac function in the mammalian myocardium. Decreased systolic Ca^{2+} release from the sarcoplasmic reticulum (SR) and increased diastolic Ca^{2+} concentration are the main features of heart failure (HF).

Cardiac SR Ca^{2+}-ATPase (SERCA2a) is responsible for most of the Ca^{2+} removal during diastole and is a larger Ca^{2+} handling energy consumer in excitation–contraction (E–C) coupling. Overexpression of SERCA2a has been suggested to be a strategic intervention for cardiac failure.

Contractile dysfunction in HF [1, 2] has been related to defective SR Ca^{2+} uptake in animal models [3] and humans [4]. Direct relationships between impaired force–frequency relation (FFR) [5], intracellular Ca^{2+} transients ($[Ca^{2+}]_i$) [6], SR Ca^{2+} content [7, 8], and SERCA2a expression [9] have also been reported in human HF. SERCA2a appears to play a key role in Ca^{2+} homeostasis, but little information on the effect of long-term SERCA2a overexpression on the mechanical work and energetics of the whole heart is available.

Previous studies with SERCA2a-overexpressing transgenic mice [10, 11] and adenovirus-mediated gene transfer in neonatal rat myocytes [12] and in rat models of HF [13–15] revealed enhanced contractility. More recent studies have reported that transgenic SERCA2a overexpression in rat hearts leads to improved relaxation and contractility under normal and pressure overload conditions [16, 17]. However, no detailed quantitative analyses of changes in Ca^{2+} handling in E–C coupling (ECC) at a whole-heart level have yet been performed. On the other hand, excessive SERCA2a-overexpression may even decrease contractility due to immediate Ca^{2+} reuptake before troponin C binding can occur, such as in the case of excessive SERCA1a-overexpression ("futile" Ca^{2+} cycling) [18].

The aim of this study was to perform a detailed analysis of the effects of long-term SERCA2a overexpression on cardiac mechanical work and energetics under physiological conditions at the whole-heart level. To attain conditions of long-term SERCA2a overexpression, we established a line of SERCA2a transgenic (TG) Wistar rats and analyzed cardiac mechanical work and energetics in excised blood-perfused TG and non-TG littermate [wildtype (WT)] hearts using our original cross-circulation system at a pacing of 300 beats/min (bpm). We were able to perform quantitative analyses—through indirect measurements—of changes in the efficiency of cross-bridge cycling and in Ca^{2+} handling energy expenditure in ECC because SERCA2a is a larger Ca^{2+} handling energy consumer in ECC.

Materials and methods

Construction of transgenic rats

Vetter et al. [19] established transgenic rat lines carrying, in addition to the endogenous SERCA2 gene, the rat SERCA2a cDNA under the control of a human cytomegalovirus immediate early enhancer (hCMV enhancer) linked to the chicken β-actin (cβA) promotor. In the current study, we used the same construct (Fig. 1). A detailed description of the latter is given in an earlier work [11] where it was used to generate SERCA2 transgenic mice.

Crj:Wistar female rats (8–12 weeks old; Charles River Japan, Kanagawa, Japan) were induced to superovulate by consecutive intraperitoneal injections of 20 IU equine chorionic gonadotropin (Serotropin; Aska Pharmaceutical, Minato-ku, Tokyo, Japan) and 10 IU human chorionic gonadotropin (Gonatropin; Aska Pharmaceutical), with a 4-h interval between injections, and mated with fertile male rats of the same strains. Pronuclear stage zygotes were collected from the oviductal ampullae 30 h after the hCG injection. The zygotes were microinjected with the exogenous DNA solution (the 6.3-kb SERCA2 expression unit) at a final concentration of 5 ng/μl and cultured for 14 h at 37°C in 5% CO_2 in air. Morphologically normal zygotes at the two-cell stage and non-degenerating one-cell stage, harvested at 14 h post-DNA microinjection, were transferred into the oviducts of recipient Wistar rats which had been previously mated with a vasectomized male rat. Embryo transfer to the pseudopregnant recipients was performed on the day that a vaginal plug was detected. Three weeks later, the pregnant recipients were allowed to deliver the offspring. The integration of exogenous DNA into rat offspring was determined by PCR analysis using genomic DNA extracted from their tail tissues and oligonucleotide primer sets suitably designed for the detection of each exogenous DNA (Fig. 2a).

All surgical and experimental procedures were performed according to the Guide for the Care and Use of Laboratory Animals published by U.S. National Institutes of Health (NIH Publication No. 85-23, revised 1996), and reviewed and approved by the animal care and use committee of Nara Medical University.

Surgical preparation

Experiments were performed on 17 excised, cross-circulated rat heart preparations, as reported previously [20–25]. In each experiment, two male crj:Wistar rats, each weighing 600 ± 98 g, and one male TG or non-TG littermate (WT) rat (14–18 weeks old) were anesthetized with pentobarbital sodium (50 mg/kg, intraperitoneal) and intubated for artificial ventilation. All rats were heparinized (1,000 units intravenous). The largest rat was used as a blood supplier to extract the largest amount of blood for priming the cross-circulation tubing. The chest was opened midsternally and the blood drained via a 21-gauge needle stabbed into the left ventricle (LV). The middle-sized rat, which was larger than the heart donor rat, was used as the metabolic supporter; the bilateral common carotid arteries and right external jugular vein were cannulated with the

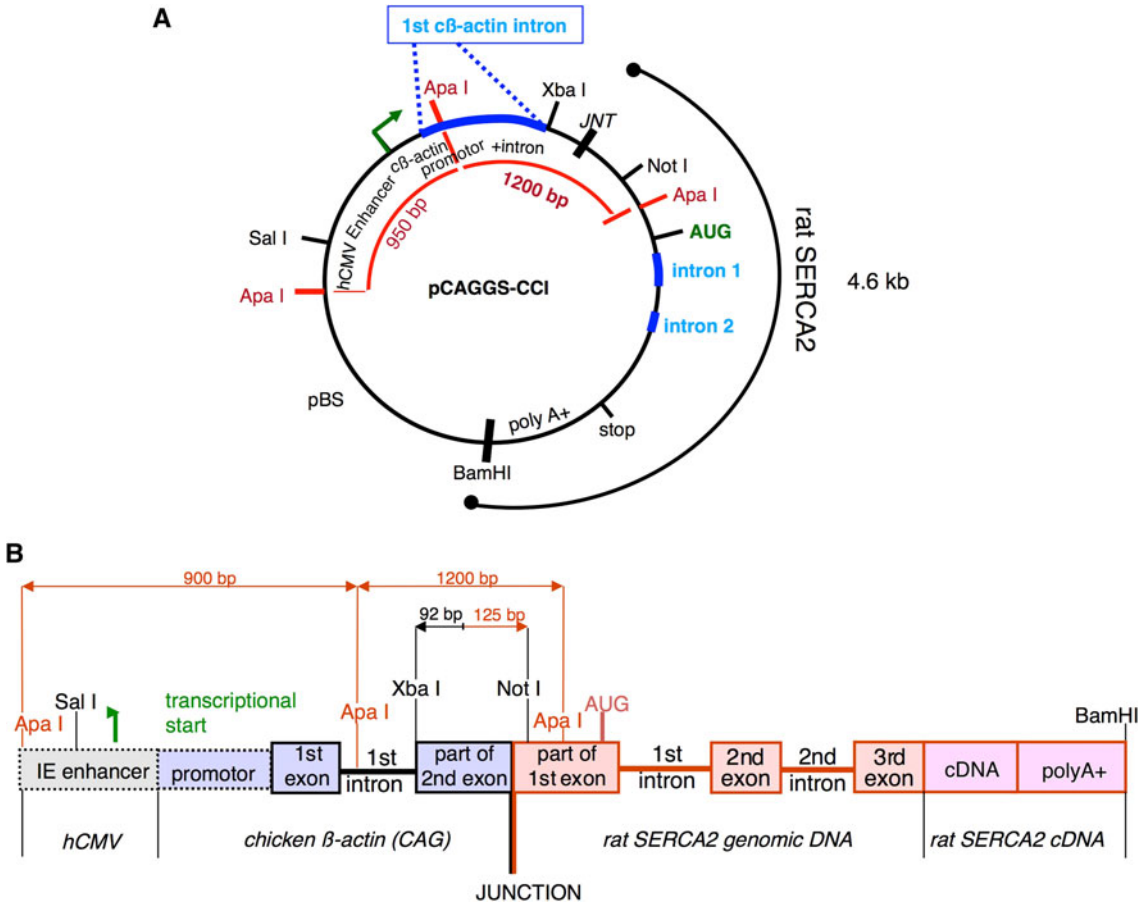

Fig. 1 The rat cardiac sarcoplasmic reticulum Ca^{2+}-ATPase (*SERCA2a*) cDNA construct used to make SERCA2a transgenic Wistar rats [19]. *cβA* Chicken *β*-actin, *hCMV* human cytomegalovirus

arterial and venous cross-circulation tubing, respectively. The chest of the smallest rat selected as the heart donor [WT, F2 (TGI) and F3 (TGII) of the same father and different mothers; Table 1] was opened midsternally under artificial ventilation. The brachiocephalic artery and the right ventricle (RV) via the superior vena cava were cannulated and connected to the arterial and venous cross-circulation tubing from the support rat. The heart–lung section was isolated from the left common carotid artery, descending aorta, inferior vena cava, and pulmonary trunk in this order. The beating heart, supported by cross circulation, was then excised from the chest. Coronary perfusion of the excised heart was never interrupted during the preparation [24]. The excised heart was maintained at 37°C.

A thin latex balloon (balloon material volume 0.08 ml) fitted into the LV was connected to a pressure transducer (Life Kit DX-312; Nihon Kohden, Tokyo, Japan) and a 0.5-ml precision glass syringe with fine scales (minimum scale 0.005 ml). The maximum unstretched balloon volume was below approximately 0.20–0.25 ml. Thus, LV volume (LVV) was changed and measured by adjusting the intra-balloon water volume with the syringe in 0.025-ml steps between 0.08 and 0.23 ml.

Systolic unstressed volume (V_0) was determined by filling the balloon to the level where peak isovolumic pressure and hence pressure–volume area (PVA) (see Data analysis) were zero. The sum of intra-balloon water volume and balloon material volume (0.08 ml) was used as an initial estimate of V_0. This procedure was repeated during different LVV-loading runs. V_0 was then finally determined as the volume–axis intercept of the best-fit end-systolic pressure–volume relationship (ESPVR). We obtained the best-fit ESPVR with $\mathrm{ESP} = A\{1 - \exp[-B(V - V_0)]\}$, and the best-fit end-diastolic pressure–volume relationship (EDPVR) with $\mathrm{ESP} = A'\{1 - [\exp(-B'(V - V_u))]^{-1}\}$ (see Table 2) by means of the least-squares method (DeltaGraph; DeltaPoint, Monterey, CA) on a personal computer [20–23, 26]. Correlation coefficients of the best-fit ESPVRs were >0.99.

The LV epicardial electrocardiogram was recorded, and the heart rate was constantly maintained by electrical

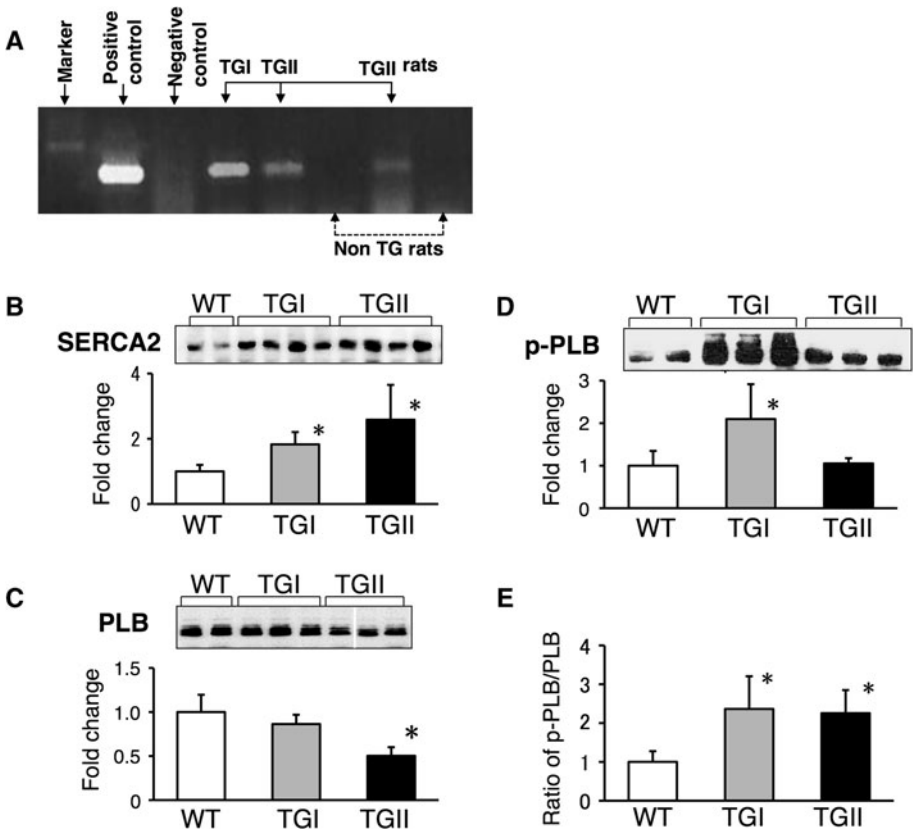

Fig. 2 Genotyping of each animal used in the study (**a**) and Western blots of SERCA2 (**b**), phospholamban (*PLB*; **c**), and phosphorylated phospholamban (*p-PLB*; **d**) in wildtype [*WT* (non-TG); $n = 8$], SERCA2a transgenic F2 (*TGI*; $n = 4$), and F3 (*TGII*; $n = 5$) rats. **e** p-PLB/PLB. $^*P < 0.05$ vs. WT

pacing of the right atrium. The pacing rate (=300 bpm) was adjusted to avoid causing incomplete relaxation or arrhythmia. The systemic arterial blood pressure of the supporter rat served as the coronary perfusion pressure (100–130 mmHg). Arterial pH, P_{O_2}, and P_{CO_2} of the supporter rat were maintained within their physiological ranges with supplemental O_2 and sodium bicarbonate.

Oxygen consumption

Total coronary blood flow was continuously measured with an electromagnetic flowmeter (MFV-3100; Nihon Kohden, Tokyo, Japan) placed in the middle of the coronary venous drainage tubing from the RV. LV thebesian flow was negligible. The coronary arteriovenous oxygen difference (AVO_2D) was continuously measured by passing all of the arterial and venous cross-circulation blood through the cuvettes of a custom-made oximeter (PWA-200S; Shoe Technica; Chiba, Japan) as previously reported in detail [20–23]. The mean concentration of hemoglobin in the perfused blood was 11.5 ± 0.6 mg/dl.

Myocardial O_2 consumption was obtained as the product of coronary flow and AVO_2D [20–22]. It was divided by pacing rate (300 bpm) to obtain O_2 consumption per beat (VO_2) in a steady state.

Lactate measurements

Blood lactate was measured with Lactate Pro (Arkray, Kyoto, Japan). The mean value of arteriovenous lactate differences at the maximum LVV loading (=the maximum O_2 demand) during vol-runs in TG rats were 0.2 ± 0.3 mM. Lactate production was negligible at the steady state of the maximum LVV loading, indicating that no ischemia occurred in our study.

Data analysis

We attempted to fit experimentally obtained LV pressure–volume data to the exponential equations to obtain ESPVRs (see Table 2) and EDPVRs. PVA is defined as the P–V area circumscribed by the curvilinear best-fit ESPVRs, EDPVRs, and the systolic portions of the ventricular P–V trajectories at any LVV. The area under the EDPVR was reasonably assumed to be zero within the same volume range. Finally, PVA was normalized by LV mass to 1 g. Based on our previous proposal in in vitro and in situ rat hearts [20, 21, 23, 27, 28], mean end-systolic pressure (ESP) at midrange LV volume (mLVV) (ESP_{mLVV}) and systolic PVA (a total mechanical energy per beat) at mLVV (PVA_{mLVV}) were calculated to assess LV mechanical work and energetics.

Table 1 Variables of body and heart weights

Variables	WT ($n = 12$)	TGI ($n = 4$)	TGII ($n = 5$)
Body weight (g)	477.5 ± 71.8	442.8 ± 67.8	423.6 ± 26.6
LV weight (g)	1.00 ± 0.12	0.82 ± 0.15*	0.81 ± 0.05*
RV weight (g)	0.28 ± 0.25	0.25 ± 0.04	0.27 ± 0.03
Heart weight/body weight (%)	0.27 ± 0.04	0.24 ± 0.01	0.26 ± 0.01
LV weight/body weight (%)	0.21 ± 0.03	0.18 ± 0.01	0.19 ± 0.01
RV weight/body weight (%)	0.06 ± 0.01	0.06 ± 0.01	0.06 ± 0.01

*$P < 0.05$ vs. WT (wildtype; non-TG)

Data are presented as the mean ± standard deviation (SD)

TGI, *TG2* cardiac sarcoplasmic reticulum Ca^{2+}-ATPase (SERCA2a) transgenic F2, F3, *LV* left ventricle, *RV* right ventricle

As shown previously [20, 21, 23–26], the VO_2–PVA relationship was linear in the rat LV. Its slope represents the O_2 cost of PVA, and its VO_2 intercept represents the PVA-independent VO_2. The PVA-independent VO_2 is composed of O_2 consumption for Ca^{2+} handling in ECC [29] and for basal metabolism [30, 31]. The RV was kept collapsed by continuous hydrostatic drainage of the coronary venous return so that the right ventricular PVA and hence PVA-dependent VO_2 were assumed to be negligible [20, 23]. The RV PVA-independent VO_2 [20, 23–26] was subtracted from the total VO_2 to yield LV VO_2. The LV (including the septum) and the RV were weighed for standardization of LVV. The data are summarized in Table 1.

Experiment protocols

Left ventricular pressure (LVP), VO_2, and PVA data during isovolumic contractions were simultaneously obtained at five to six different LVVs (EDVs) in each heart (vol-run).

After the control vol-run, a Ca^{2+}-induced different inotropic run (Ca^{2+} ino-run) was performed at mLVV [0.16 ml = 0.08 ml (a half value between minimum and maximum water volume infused into the balloon) plus 0.08 ml (V_0)] during intracoronary infusion of a 1% $CaCl_2$ solution. The infusion rate of Ca^{2+} was increased in steps up to 1–16, 1–14, and 1–30 ml/h ($n = 8$, 4 and 5 in the WT, TGI, and TGII groups) until initiation of the decrease in LV ESP or arrhythmia due to Ca^{2+} overload. Each maximum Ca^{2+} concentration calculated by infusion rate (ml/min)/coronary flow (ml/min) was 6.8 ± 1.5, 9.3 ± 1.1, and 16.1 ± 3.2 mM ($P < 0.005$ vs. WT). Tolerance to increasing Ca^{2+} concentrations in TGII was significantly higher than that in WT. In every vol-run and ino-run, LVP, AVO_2D, and CF were stable 3 min after changing the LVV and infusion rate of Ca^{2+}.

To measure basal metabolic O_2 consumption, we induced cardiac arrest by infusing KCl (0.5 M) into the coronary perfusion tubing at 5–10 ml/h ($n = 8$, 4, and 5 in each group), which was adjusted to abolish electrical excitation under monitoring ventricular electrocardiograms, but not to generate any KCl-induced constrictions of coronary vessels, by monitoring coronary flow (>1.0 ml/min) and systemic blood pressure (corresponding to perfusion pressure) in the metabolic supporter rat to check the loss of perfusion pressure dependency. VO_2 and PVA data were obtained by minimal volume loading to avoid volume-loading effects on VO_2 data. In each steady state, all data were measured and sampled at 1 kHz for 5–10 s and averaged using a PowerLab unit and Chart software (AD Instruments, Bella Vista, NSW, Australia).

Mean values for mLVV and V_0 (normalized for LV 1 g) are summarized in Table 2.

Oxygen cost of LV contractility

We obtained the specific best-fit curve for the observed ESP_{mLVV} and ESP (0 mmHg at V_0) with the best-fit ESPVR function in control vol-run by the least squares method, and we calculated PVA_{mLVV} during Ca^{2+} infusion using this specific best-fit curve function on a personal computer [22, 23, 32, 33]. The parallelism of the VO_2–PVA linear relation during Ca^{2+} infusion has been confirmed in WT and TG hearts. From this parallelism, the lines including all VO_2–PVA data obtained during Ca^{2+} infusion in steps at mLVV were drawn in parallel to the VO_2–PVA relation line before Ca^{2+} infusion, as described previously [20, 22, 32, 33]. The gradually increased VO_2–intercept values (PVA-independent VO_2 values) of the lines proportional to the enhanced LV contractility by Ca^{2+} were obtained by this procedure.

Our proposed index for LV contractility, equivalent maximal elastance (eEmax), was calculated from a triangular area equivalent to PVA_{mLVV} [23, 33]. The O_2 cost of LV contractility was the slope of the relationship between PVA-independent VO_2 and eEmax, i.e., the VO_2 used for Ca^{2+} handling in ECC per unit changes in LV contractility [23, 31, 33].

Table 2 Variables of left ventricular mechanical work at a pacing of 300 bpm

Variables	WT ($n = 8$)	TGI ($n = 4$)	TGII ($n = 5$)
ESPVR[a]			
A (mmHg)	196.2 ± 48.4	208.1 ± 40.5	199.5 ± 51.0
B (ml^{-1})	17.3 ± 9.6	23.1 ± 9.5	12.7 ± 7.3
V_0 ($\times 10^{-2}$ ml g^{-1})	8.06 ± 1.09	9.97 ± 0.70	9.46 ± 0.94
EDPVR[a]			
A' (mmHg)	0.096 ± 0.11	0.045 ± 0.053	0.069 ± 0.094
B' (ml^{-1})	40.2 ± 17.3	30.7 ± 4.3	34.4 ± 9.6
ESP_{mLVV} (mmHg)	129.3 ± 30.8	175.3 ± 36.3*, #	116.5 ± 21.9
PVA_{mLVV} (mmHg ml $beat^{-1}$ g^{-1})	6.55 ± 2.10	12.36 ± 4.26*, #	7.02 ± 2.77
mLVV (ml g^{-1})	0.166 ± 0.022	0.200 ± 0.037	0.189 ± 0.018

*$P < 0.05$ vs. WT; #$P < 0.05$ versus TGII

Values are presented as the mean ± SD

mLVV midrange left ventricular volume, ESP_{mLVV} end-systolic pressure at mLVV, PVA_{mLVV} systolic pressure–volume area at mLVV, V_0 volume intercept of ESPVR normalized by LV mass to 1 g

[a] A, B, Parameters of best-fit end-systolic pressure–volume relation (ESPVR) obtained by $ESP = A\{1 - \exp[-B(V - V_0)]\}$; A', B' parameters of best-fit end-diastolic pressure–volume relation (EDPVR) obtained by $ESP = A'\{1 - [\exp(-B'(V - V_u))]^{-1}\}$. Each best-fit curve was obtained by ESP-V data during left ventricular (LV) volume-loading run

Ca^{2+} overloading protocol

To obtain Ca^{2+}-overloaded acute failing hearts to observe mitochondrial swelling at the electron microscopic (EM) level, we increased the infusion rate of the 5% $CaCl_2$ solution into the coronary circulation in steps up to 5–6 ml/h at mLVV. The blood Ca^{2+} concentration ultimately reached approximately 12 mM.

Analyses of one-beat LV pressure–time curve by hybrid and single logistic functions

To evaluate LV end-diastolic relaxation rate or lusitropism, we analyzed the "logistic" time constant (T_L) from respective best-fit functions to the one-beat LV pressure–time curve at mLVV during relaxation with our proposed "single logistic function" [34] in WT ($n = 8$), TGI ($n = 4$), and TGII ($n = 5$) group hearts under control and 1% $CaCl_2$ solution-infused conditions at the rate of 8 ml/h.

Ultrastructural observations

For EM examination, we prepared two different hearts: WT rat hearts that had undergone the Ca^{2+} overloading protocol ($n = 2$) and SERCA2a transgenic (TGII) rat hearts that had undergone the Ca^{2+} overloading protocol ($n = 2$). Each heart was removed from the rat and submerged in a bath of ice-cold fixative solution containing 2.5% glutaraldehyde in 0.1 M phosphate buffer, pH 7.4. The first step consisted of cutting small and transmural samples of the epicardium and endocardium from the lateral wall of the LV and fixing these in the same fixative for conservation. We then cut the sample perpendicularly to the epicardium with a sharp blade to separate well-fixed, outer surface layers of 1-mm thickness from the core of the tissue block and further fixed these outer thin slices in the same fresh fixative at 4°C for 4 h. After being rinsed with the same buffer, the specimens were post-fixed for 3 h with 1.0% OsO_4 in 0.1 M phosphate buffer, pH 7.4, dehydrated through an ascending series of ethanol and substituted with propylene oxide, and finally embedded in epoxy resin. Ultrathin sections were cut, stained with uranyl acetate and lead citrate, and observed in an electron microscope (JEM1200 EXII; JEOL, Tokyo, Japan).

Polyacrylamide gel electrophoresis and western blots for SERCA2a, phospholamban and phospho-Ser^{16}PLB

Membrane proteins were isolated from the LV wall of each frozen heart. The frozen hearts were first homogenized and centrifuged at 1,000 *g* for 10 min, and the resulting supernatants were further centrifuged at 100,000 *g* for 60 min at 4°C. The pellets obtained after this latter step comprised cellular membrane fractions and were used for immunoblotting of SERCA2a, monomeric phospholamban (PLB), and phospho-Ser^{16}PLB (p-PLB).

The same amounts of membrane proteins (10 μg/lane) were separated on sodium dodecyl sulfate-polyacrylamide gels (10% for SERCA2, 15% for PLB and p-PLB) in a minigel apparatus (Mini-PROTEAN II; Bio-Rad, Hercules, CA), and transferred to polyvinylidene difluoride membranes. The membranes were blocked (4% Block Ace; Dainippon Pharmaceutical, Osaka, Japan) and then incubated with anti-SERCA2a antibody (1:1000 dilution;

Affinity Bioreagents, Rockford, IL), anti-PLB antibody (1:2000 dilution; Upstate Biotechnology, Lake Placid, NY), and anti-p-PLB (Ser^{16}) antibody (1:1000 dilution; Upstate Biotechnology). The antigens were detected by the luminescence method (ECL Western blotting detection kit; Amersham, Arlington Heights, IL) with peroxidase-linked anti-mouse immunoglobulin G (IgG) (1:2000 dilution) or peroxidase-linked anti-rabbit IgG (1:2000 or 1:5000 dilution). After immunoblotting, the film was scanned with a scanner, and the intensity of the bands was calculated by NIH image analysis.

Statistics

Multiple comparisons were performed by one-way analysis of variance (ANOVA) with post hoc Bonferroni's test or Fisher's PLSD test. A value of $P < 0.05$ was considered statistically significant. All data are expressed as the mean ± standard deviation.

Results

Cardiac weights

Body weights in the WT, TGI, and TGII groups were not significantly different. RV weight, and LV and RV weight ratios to body weight in the WT, TGI, and TGII groups were not significantly different, but LV weight in the TGI and TGII groups was significantly smaller than that in the WT (Table 1). These data are substantially the same as those previously reported by Maier et al. [16]. We also measured echocardiographic data in in vivo hearts of the WT, TGI, and TGII groups. According to these data, the wall thickness parameter and functional parameters were not significantly different among the three groups (data not shown).

Western blotting of SERCA2a and PLB

We confirmed the expression of SERCA2a genes in the TG rats (Fig. 2a). SERCA2 protein expression increased significantly but moderately in TGI rats compared to that in the WT; the relative increase in TGII rats was larger (Fig. 2b). PLB protein expression was significantly decreased in TGII rats (Fig. 2c), but the ratios of p-PLB/PLB in both the TGI and TGII groups were significantly increased compared to that in the WT group although there were no differences in the ratios between the TGI and TGII groups(Fig. 2e).

ESPVRs and VO_2–PVA relations

Figure 3 shows representative ESPVR, EDPVR, and VO_2–PVA relations in WT, TGI, and TGII rats. An ESPVR in the TGI group (red curve in Fig. 3a; color figure online) shifted upward from that in the WT group, and an ESPVR in the TGII group (blue curve in Fig. 3a) was similar to that in the WT group (black curve in Fig. 3a). Each slope of two VO_2–PVA relations in TGI and TGII rats was smaller than that in the WT, whereas each VO_2 intercept in the TGI and TGII groups was slightly larger than that in the WT group(Fig. 3b). Summarized data of LV mechanics are shown in Table 2. Although best-fit parameters for ESPVR were not significantly different among the three groups, mean ESP_{mLVV} and PVA_{mLVV} in the TGI group were significantly larger than those in the WT and TGII groups.

The mean slopes of the VO_2–PVA relationships in the TGI and TGII groups were significantly smaller than that in the WT group (Fig. 4a), and the mean VO_2 intercepts (PVA-independent VO_2) of the VO_2–PVA relationships were not significantly different among the three groups (Fig. 4b). The VO_2 intercept was composed of oxygen consumption for Ca^{2+} handling in ECC and for basal metabolism. The mean oxygen consumption for Ca^{2+}

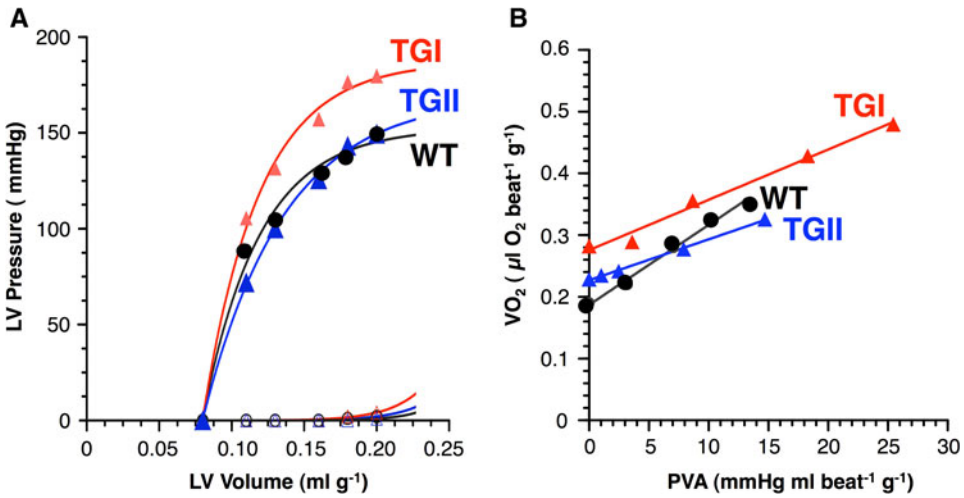

Fig. 3 Representative left ventricular (*LV*) end-systolic pressure–volume relations (ESPVRs), end-diastolic pressure–volume relations (EDPVRs) (**a**) and myocardial oxygen consumption per beat (VO_2)–systolic pressure–volume area (*PVA*; a total mechanical energy per beat) relations (**b**) in the WT, TGI and TGII groups. WT *black circle*, TGI *blue triangle*, TGII *red triangle*. (Color figure online)

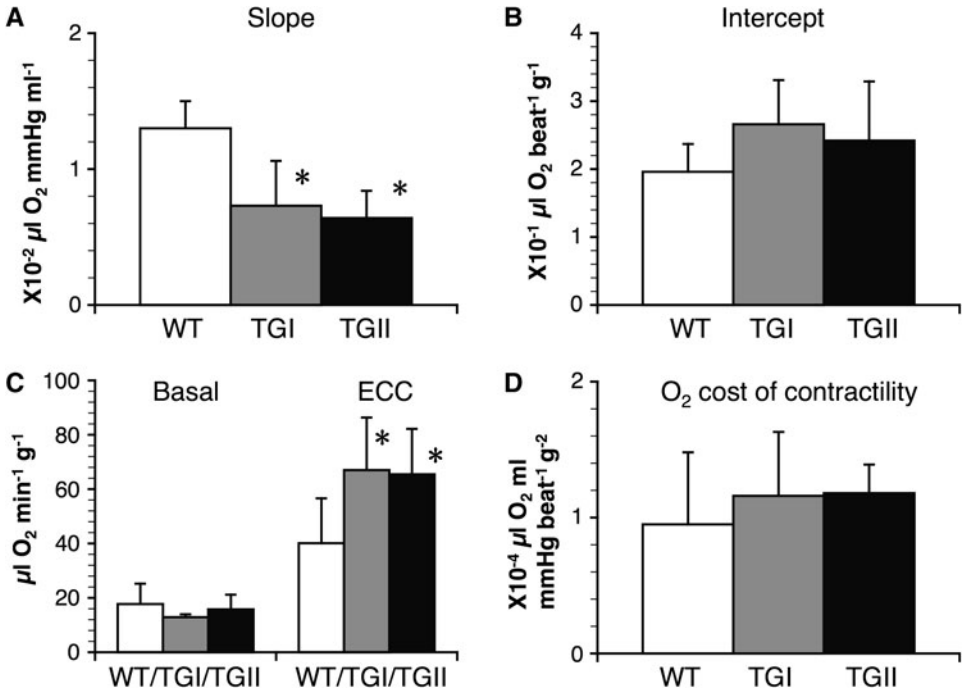

Fig. 4 Summary of mean slope (**a**) and VO_2 intercept (**b**) of the VO_2–PVA relations, oxygen consumption per minute for basal metabolism (*Basal*) and excitation–contraction (E–C) coupling (*ECC*) (**c**) and O_2 cost of LV contractility (**d**) in the WT ($n = 8$), TGI ($n = 4$), and TGII ($n = 5$) groups. $^*P < 0.05$ vs. WT

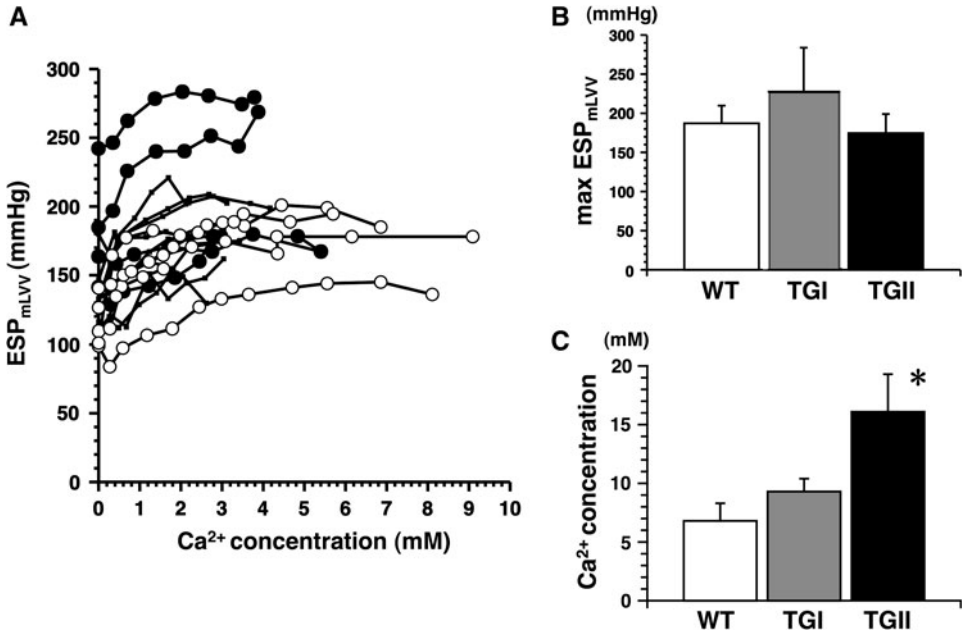

Fig. 5 All end-systolic pressure at midrange LVV (ESP_{mLVV})–Ca^{2+} concentration relations (**a**), mean maximum ESP_{mLVV} (**b**) and mean maximum Ca^{2+} concentration infused (**c**) in the WT ($n = 8$), TGI ($n = 4$) and TGII ($n = 5$) groups. *LVV* Left ventricular volume. $^*P < 0.05$ vs. WT. **a** WT *small filled square*, TGI *large filled circle*, TGII *large open circle*

handling in ECC per minute (=$VO_2 \times 300$ bpm − basal metabolism per minute) in the TGI and TGII groups was significantly larger than that in the WT group, whereas the mean oxygen consumption for basal metabolism per minute was not different among the three groups (Fig. 4c).

Oxygen cost of LV contractility

Each maximum Ca^{2+} concentration–maximum ESP_{mLVV} relation during Ca^{2+} infusion is shown in Fig. 5a. Although the mean maximal ESP_{mLVV} was not significantly different among the three groups (Fig. 5b), the mean maximum Ca^{2+} concentration in the TGII group was significantly ($P < 0.05$) higher than that in the WT group (Fig. 5c), indicating a higher tolerance to increasing Ca^{2+} concentration in the TGII group (see Experiment protocols). This result may support the possibility for SERCA2a-overexpression in TGII.

A representative PVA-independent VO_2 and $eEmax_{mLVV}$ linear relation in each three group is shown in Fig. 5. Each PVA-independent VO_2 and $eEmax_{mLVV}$ relation was in parallel, indicating unchanged oxygen cost of LV

contractility for Ca^{2+} in the WT, TGI, and TGII groups (Fig. 6). The mean oxygen costs of LV contractility for Ca^{2+} were not different among the three groups (Fig. 4d).

Logistic time constant

The mean logistic time constant (T_L) was not significantly different among the three groups under control conditions (1% $CaCl_2$ solution infused at 0 ml/h) at 300 bpm, indicating that the end-diastolic relaxation rate in the three groups was similar. Under the 1% $CaCl_2$ solution infused at 8 ml/h condition, mean T_L became slightly shorter than those under control conditions in each group, although there were no significant differences among the three groups (data not shown).

Electron microscopy

At the ultrastructural level, there were no particular alterations in TGII hearts which underwent the Ca^{2+} overloading protocol (Fig. 7a). The myocytes of all groups had relaxed sarcomeres and intact sarcolemmal membranes. There was no disintegration of muscle myofibrils. The mitochondria, SR, and t-tubules were intact. In WT hearts which underwent the same Ca^{2+} overloading protocol, slightly swollen mitochondria were noted in a part of the myocytes (Fig. 7b). Other organelles were intact.

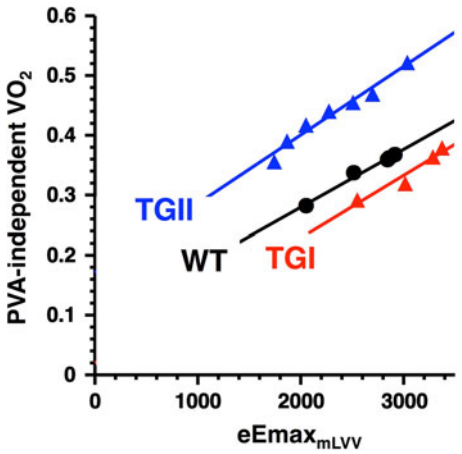

Fig. 6 Representative PVA-independent VO_2-equivalent maximal elastance at mLVV ($eEmax_{mLVV}$) relations in the WT, TGI and TGII groups. WT *black circle*, TGI *red triangle*, TGII *blue triangle*. (Color figure online)

Discussion

In the transgenic rat hearts studied here, LV systolic function indicated by ESP_{mLVV} and PVA_{mLVV} was enhanced in the TGI group or unchanged in TGII group, although LV diastolic function was not different among the WT, TGI and TGII groups. The slope of the VO_2–PVA relationship in the TG group was smaller than that in the WT group at a pacing of 300 bpm. The VO_2 intercept of the VO_2–PVA relationship was slightly higher, but not significantly different, and the O_2 costs of LV contractility were not significantly different among the three groups. However, the mean oxygen consumption for Ca^{2+} handling in ECC per minute in the TG group was significantly larger than that in the WT group, whereas the mean oxygen consumption for basal metabolism per minute was not different among the three groups. The increased mean oxygen consumption for Ca^{2+} handling in ECC per minute indicates SERCA2a hyperactivity.

VO_2–PVA relation

The small slope of the VO_2–PVA relation indicated the smaller oxygen cost of PVA. The smaller oxygen cost of PVA means that the ratio of chemo–mechanical energy transduction is higher based on the theoretical background [31]. The reciprocal of the slope of the VO_2–PVA relation has been considered to be the contractile efficiency, which reflects the chemo–mechanical energy transduction efficiency of the contractile machinery, and to be the product of the efficiency from VO_2 to ATP (mitochondrial oxidative phosphorylation) and the efficiency from ATP to PVA (cross-bridge cycling) [31]. Therefore, the efficiency of cross-bridge cycling appears to be higher in TG rat hearts at 300 bpm.

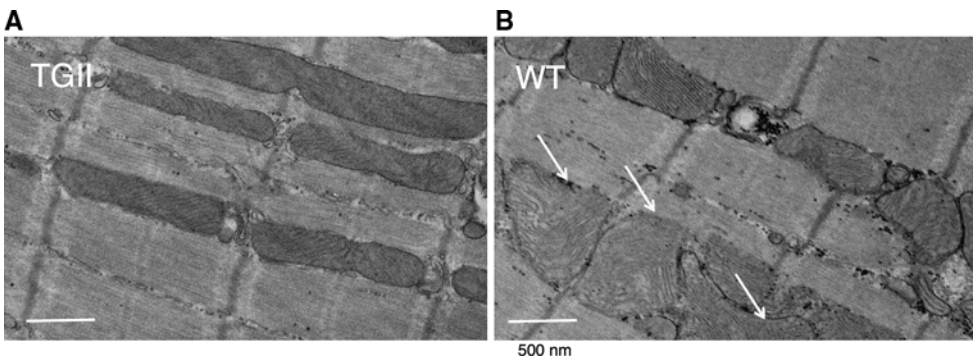

Fig. 7 Mitochondrial swelling was not observed in electron micrographs of myocytes in TG hearts (**a**) but was observed in WT hearts (**b**) under Ca^{2+} overloaded conditions. *Arrows* indicate slightly swollen mitochondria in the Ca^{2+} overloaded WT myocyte. *Bars* 500 nm

Oxygen cost of LV contractility

It is predicted that SERCA2a protein overexpression in TG rats increases the Ca^{2+} recycling fraction through SERCA2a and consequently decreases Ca^{2+} extrusion via the Na^{+}–Ca^{2+} exchanger (NCX). This prediction is in consistent with data reported by Maier et al. [16] showing that SR Ca^{2+} loading was increased, whereas transsarcolemmal Ca^{2+} fluxes were decreased, in single myocytes of similar SERCA2a-overexpressing TG rats. Although NCX per se does not consume ATP to remove cytosolic Ca^{2+} in exchange for incoming Na^{+} on the basis of a stoichiometry of $3Na^{+}$:$1Ca^{2+}$, the incoming Na^{+} will be pumped out by Na^{+}–K^{+}–ATPase with a stoichiometry of $3Na^{+}$:$2K^{+}$:1ATP, resulting in the net stoichiometry of $1Ca^{2+}$:1ATP [35]. SERCA2a removes cytosolic Ca^{2+} on the basis of a stoichiometry of $2Ca^{2+}$:1ATP. Therefore, increases in the Ca^{2+} recycling fraction through SERCA2a leads to a decrease in energy expenditure compared with the Ca^{2+} extrusion by NCX if the same amount of Ca^{2+} is handled. However, this did not occur in the blood-perfused whole-heart preparations of the TG rats in our study. Our data indicate an overall maintained oxygen cost of LV contractility.

In WT rats, SERCA2a activity is sufficiently high at a pacing of 300 bpm because of a large concentration of SERCA2a molecules, and Ca^{2+} removal via NCX is low; this results in a balance of 92% for SERCA2a, 7% for NCX, and 1% for sarcolemmal Ca^{2+}–ATPase and mitochondrial Ca^{2+} uniporter [35–38]. Our results in TG rats show increased O_2 consumption for Ca^{2+} handling in ECC per minute, which is expected since the machinery is overactive, but the overall O_2 cost for LV contractility is unchanged. This parameter may suggest that the energy cost of the Ca^{2+} reuptake is balanced, resulting in normal costs of energy expenditure. The data indicate an overall maintained oxygen cost of LV contractility.

At each Ca^{2+} concentration, the response of the ESP_{mLVV} relation in the three groups indicated that the TGII heart seems to have tolerated higher Ca^{2+} concentrations. The mean Ca^{2+} concentration inducing maximal ESP_{mLVV} in the TGII group was significantly higher than that in the WT group (see Fig. 5c). Tolerance to higher Ca^{2+} concentrations may support the possibility for SERCA2a overexpression in the TGII heart.

At the EM levels, there were no particular differences in TGII hearts that underwent the Ca^{2+} overloading protocol versus the WT hearts which underwent the same protocol, where slightly swollen mitochondria were noted. This observation indicates that increasing SR Ca^{2+} pump function prevented the TG hearts from mitochondrial swelling, resulting in cardiac protection.

It has been reported that increasing SR Ca^{2+} pump function is not beneficial in the normal heart model with normal SERCA2a levels [18]. However, increasing SR Ca^{2+} pump function will be beneficial in the cardiac failure model with a downregulated SERCA2a level [39]. As a next study, we are planning to study the isoproterenol-induced failing heart model of TG rats because the SERCA2a level is downregulated in this model [40].

Although previous studies have shown improved myocardial function and improved (or spared) energetic consumption with gene transfer of SERCA2a under acute conditions [12–14, 41], chronic studies addressing the long-term effect of targeting calcium reuptake are lacking. In conclusion, the data from our study suggest that long-term SERCA2a overexpression enhances or maintains LV mechanics and improved contractile efficiency under higher energy expenditure for Ca^{2+} handling in ECC and Ca^{2+} tolerance, but that it does not change the overall O_2 cost of LV contractility for Ca^{2+} in normal hearts of TG rats at 300 bpm.

Acknowledgments This work was supported in part by Grants-in-Aid No. 22790216 for Scientific Research from the Ministry of Education, Culture, Sports, Science and Technology of Japan.

References

1. Gwathmey JK, Copelas L, MacKinnon R, Schoen FJ, Feldman MD, Grossman W, Morgan JP (1987) Abnormal intracellular Ca^{2+} handling in myocardium from patients with end-stage heart failure. Circ Res 61:70–76
2. Hasenfuss G, Mulieri LA, Leavitt BJ, Allen PD, Haeberle JR, Alpert NR (1992) Alteration of contractile function and excitation–contraction coupling in dilated cardiomyopathy. Circ Res 70:1225–1232
3. Hasenfuss G (1998) Animal models of human cardiovascular disease, heart failure and hypertrophy. Cardiovasc Res 39:60–76
4. Hasenfuss G, Pieske B (2002) Calcium-cycling in congestive heart failure. J Mol Cell Cardiol 34:951–969
5. Pieske B, Kretschmann B, Meyer M, Holubarsch C, Weirich J, Posival H, Minami K, Just H, Hasenfuss G (1995) Alterations in intracellular calcium handling associated with the inverse force–frequency relation in human dilated cardiomyopathy. Circulation 92:1169–1178
6. Beuckelmann DL, Näbauer M, Erdmann E (1992) Intracellular calcium handling in isolated ventricular myocytes from patients with terminal heart failure. Circulation 85:1046–1055
7. Lindner M, Erdmann E, Beuckelmann DJ (1998) Calcium-content of SR in isolated ventricular myocytes from patients with terminal heart failure. J Mol Cell Cardiol 30:743–749
8. Pieske B, Maier LS, Bers DM, Hasenfuss G (1999) Ca^{2+}-handling and SR Ca^{2+}-content in isolated failing and nonfailing human myocardium. Circ Res 85:38–46
9. Hasenfuss G, Reinecke H, Studer R, Meyer M, Pieske B, Holtz J, Holubarsch C, Posival H, Just H, Drexler H (1994) Relation between myocardial function and expression of SR Ca^{2+}-ATPase in failing and nonfailing human myocardium. Circ Res 75:434–442
10. Baker DL, Hashimoto K, Grupp IL, Ji Y, Reed T, Loukianov E, Grupp G, Bhagwhat A, Hoit B, Walsh R, Marban E, Periasamy M (1998) Targeted overexpression of the SR Ca^{2+}-ATPase

increases cardiac contractility in transgenic mouse hearts. Circ Res 83:1205–1214
11. He H, Giordano FJ, Hilal-Dandan R, Choi DJ, Rockman HA, McDonough PM, Bluhm WF, Meyer M, Sayen MR, Swanson E, Dillmann WH (1997) Overexpression of the rat sarcoplasmic reticulum Ca^{2+} ATPase gene in the heart of transgenic mice accelerates calcium transients and cardiac relaxation. J Clin Invest 100:380–389
12. Giordano FJ, He H, McDounough P, Meyer M, Sayen MR, Dillmann WH (1997) Adenovirus-mediated gene transfer reconstitutes depressed SR Ca^{2+}-ATPase levels and shortens prolonged cardiac myocyte Ca^{2+}-transient. Circulation 96:400–403
13. del Monte F, Williams E, Lebeche D, Schmidt U, Rosenzweig A, Gwathmey JK, Lewandowski ED, Hajjar RJ (2001) Improvement in survival and cardiac metabolism after gene transfer of SR Ca^{2+}-ATPase in a rat model of heart failure. Circulation 104:1424–1429
14. Miyamoto MI, del Monte F, Schmidt U, DiSalvo TS, Kang ZB, Matsui T, Guerrero JL, Gwathmey JK, Rosenzweig A, Hajjar RJ (2000) Adenoviral gene transfer of SERCA2a improves left ventricular function in aortic-banded rats in transition to heart failure. Proc Natl Acad Sci USA 97:793–798
15. Schmidt U, del Monte F, Miyamoto MI, Matsui T, Gwathmey JK, Rosenzweig A, Hajjar RJ (2000) Restoration of diastolic function in senescent rat hearts through adenoviral gene transfer of SR Ca^{2+}-ATPase. Circulation 101:790–796
16. Maier LS, Wahl-Schott C, Horn W, Weichert S, Pagel C, Wagner S, Dybkova N, Müller OJ, Näbauer M, Franz W-M (2005) Increased SR Ca^{2+} cycling contributes to improved contractile performance in SERCA2a-overexpressing transgenic rats. Cardiovasc Res 67:636–646
17. Müller OJ, Lange M, Rattunde H, Lorenzen H-P, Müller M, Frey N, Bittner C, Simonides W, Katus HA, Franz W-M (2003) Transgenic rat hearts overexpressing SERCA2a show improved contractility under baseline conditions and pressure overload. Cardiovasc Res 59:380–389
18. Teucher N, Prestle J, Seidler T, Currie S, Elliott EB, Reynolds DF, Schott P, Wagner S, Kogler H, Inesi G, Bers DM, Hasenfuss G, Smith GL (2004) Excessive sarcoplasmic/endoplasmic reticulum Ca^{2+}-ATPase expression causes increased sarcoplasmic reticulum Ca^{2+} uptake but decreases myocyte shortening. Circulation 110:3533–3559
19. Vetter R, Rehfeld U, Reissfelder C, Weiß W, Wagner K-D, Günther J, Hammes A, Tschöpe C, Dillmann W, Paul M (2002) Transgenic overexpression of the sarcoplasmic reticulum Ca^{2+} ATPase improves reticular Ca^{2+} handling in normal and diabetic rat hearts. FASEB J 16:1657–1659
20. Hata Y, Sakamoto T, Hosogi S, Ohe T, Suga H, Takaki M (1998) Linear O_2 use–pressure–volume area relation from curved end-systolic pressure–volume relation of the blood-perfused rat left ventricle. Jpn J Physiol 48:197–204
21. Hata Y, Sakamoto T, Hosogi S, Ohe T, Suga H, Takaki M (1998) Effects of thapsigargin and KCl on the O_2 use of the excised blood perfused rat heart. J Mol Cell Cardiol 30:2137–2144
22. Tsuji T, Ohga Y, Yoshikawa Y, Sakata S, Abe T, Tabayashi N, Kobayashi S, Kitamura S, Taniguchi S, Suga H, Takaki M (2001) Rat cardiac contractile dysfunction induced by Ca^{2+} overload: possible link to the proteolysis of fodrin. Am J Physiol Heart Circ Physiol 281:H1286–H1294
23. Tsuji T, Ohga Y, Yoshikawa Y, Sakata S, Kohzuki H, Misawa H, Abe T, Tabayashi N, Kobayashi S, Kitamura S, Taniguchi S, Suga H, Takaki M (1999) New index for oxygen cost of contractility from curved end-systolic pressure–volume relations in cross-circulated rat hearts. Jpn J Physiol 49:513–520
24. Yoshikawa Y, Hagihara H, Ohga Y, Nakajima-Takenaka C, Murata K, Taniguchi S, Takaki M (2005) Calpain inhibitor-1 protects the rat heart from ischemic–reperfusion injury: analysis by mechanical work and energetics. Am J Physiol Heart Circ Physiol 288:H1690–H1698
25. Yoshikawa Y, Zhang G-X, Obata K, Ohga Y, Matsuyoshi H, Taniguchi S, Takaki M (2010) Cardioprotective effects of a novel calpain inhibitor SNJ-1945 for reperfusion injury after cardioplegic cardiac arrest. Am J Physiol Heart Circ Physiol 298:H643–H651
26. Abe T, Ohga Y, Tabayashi N, Kobayashi S, Sakata S, Misawa H, Tsuji T, Kohzuki H, Suga H, Taniguchi S, Takaki M (2002) Left ventricular diastolic dysfunction in type 2 diabetes mellitus model rats. Am J Physiol Heart Circ Physiol 282:H138–H148
27. Lee S, Ohga Y, Tachibana H, Syuu Y, Ito H, Harada M, Suga H, Takaki M (1998) Effects of myosin isozyme shift on curvilinearity of the left ventricular end-systolic pressure–volume relation of in situ rat hearts. Jpn J Physiol 48:445–455
28. Tachibana H, Takaki M, Lee S, Ito H, Yamaguchi H, Suga H (1997) New mechanoenergetic evaluation of left ventricular contractility in in situ rat hears. Am J Physiol Heart Circ Physiol 272:H2671–H2678
29. Takaki M, Kohzuki H, Kawatani Y, Yoshida A, Ishidate H, Suga H (1998) Sarcoplasmic reticulum Ca^{2+} pump blockade decreases O_2 use of unloaded contracting rat heart slices: thapsigargin and cyclopiazonic acid. J Mol Cell Cardiol 30:649–659
30. Ohga Y, Sakata S, Takenaka C, Abe T, Tsuji T, Taniguchi S, Takaki M (2002) Cardiac dysfunction in terms of left ventricular mechanical work and energetics in hypothyroid rats. Am J Physiol Heart Circ Physiol 283:H631–H641
31. Takaki M (2004) Left ventricular mechanoenergetics in small animals. Jpn J Physiol 54:175–207
32. Sakata S, Ohga Y, Abe T, Tabayashi N, Kobayashi S, Tsuji T, Kohzuki H, Misawa H, Taniguchi S, Takaki M (2001) No dependency of a new index for oxygen cost of left ventricular contractility on heart rates in the blood-perfused excised rat heart. Jpn J Physiol 51:177–185
33. Tabayashi N, Abe T, Kobayashi S, Yoshikawa Y, Sakata S, Takenaka C, Misawa H, Taniguchi S, Takaki M (2002) Oxygen costs of left ventricular contractility for dobutamine and Ca^{2+} in normal rat hearts and the cost for dobutamine in Ca^{2+} overload-induced failing hearts. Jpn J Physiol 52:163–171
34. Matsubara H, Takaki M, Yasuhara S, Araki J, Suga H (1995) Logistic time constant of isovolumic relaxation pressure–time curve in the canine left ventricle: better alternative to exponential time constant. Circulation 92:2318–2326
35. Bers DM (2000) Calcium fluxes involved in control of cardiac myocyte contraction. Circ Res 87:275–281
36. Bers DM (2001) Excitation–contraction coupling and cardiac contractile force, 2nd edn. Kluwer, Dordrecht
37. Bers DM (2002) Cardiac excitation–contraction coupling. Nature 415:198–205
38. Bers DM (2002) Cardiac Na/Ca exchange function in rabbit, mouse and man: what's the difference? J Mol Cell Cardiol 34:369–373
39. Vetter R, Rehfeld U, Reissfelder R, Fechner H, Seppet E, Kreutz R (2010) Decreased cardiac SERCA2 expression, SR Ca uptake, and contractile function in hypothyroidism are attenuated in SERCA2 overexpressing transgenic rats. Am J Physiol Heart Circ Physiol 300:H943–H950
40. Nakajima-Takenaka C, Zhang GX, Obata K, Tohne K, Matsuyoshi H, Nagai Y, Nishiyama A, Takaki M (2009) Left ventricular function of isoproterenol-induced hypertrophied rat hearts perfused with blood: mechanical work and energetics. Am J Physiol Heart Circ Physiol 297:H1736–H1743
41. Hajjar RJ, Kang JX, Gwathmey JK, Rosenzweig A (1997) Physiological effects of adenoviral gene transfer of sarcoplasmic reticulum calcium ATPase in isolated rat myocytes. Circulation 95:423–429